Submitted to ADVANCED MATERIALS

DOI: 10.1002/adma.((please add manuscript number))

A gold marker technique revealing phase-specific wear and sub-surface deformation with nanometer resolution

By Dmitry Shakhvorostov*, Peter R. Norton, and Martin H. Müser

[*] Dr. D. Shakhvorostov, Prof. M.H. Müser,
Universität des Saarlandes, Lehrstuhl für Materialsimulation,
Campus, C 6.3, Saarbrücken, 66123 Germany
E-mail: dshakh@mx.uni-saarland.de

Prof. P. R. Norton
University of Western Ontario, Department of Chemistry,
1151 Richmond St. N., London, ON, N6A 5B7 Canada

Keywords: Wear, GMT, Gold Marker Technique, Aluminum-Silicon Alloy

Understanding the mechanisms of wear can potentially lead to the development of new materials and processes that can increase the life span of devices and machines with moving parts.[1] Simple approaches such as increasing the macro-hardness of materials, no longer suffice, [2] as the ongoing miniaturization of devices and their increasing energy throughput, demand new concepts requiring an understanding of wear mechanisms at the nanoscale,[3,4,5,6,7] for which macro-hardness is not a reliable indicator.

Currently most experiments yield the amount of worn material as a function of load and sliding distance. While such experiments will always remain important for benchmarking of specific materials and lubricants, they can only yield an incomplete picture of wear *mechanisms* in the absence of micro- and nanoscale imaging. Early wear measurements involved weighing objects before and after rubbing,[1] but these methods require one to stop the experiment for data acquisition. By contrast, new methods involving chemical analysis [8,9,10,11,12,13,14] as well as the radioactive tracer technique (RTT) [15,16,17,18,19,20] or radionuclide technique (RNT) [21] can measure wear as a function of time, but these methods are only sensitive to mass differences, but insensitive to worn but unremoved material. They also generally lack (high) spatial resolution.

In modern, spatially resolved wear measurements, the volume of worn, detached, and deformed material is quantified by comparing topographies of the originally unworn and the later worn solid. The most commonly used methods are optical and atomic force microscopies. Unlike mass-sensitive methods, these new techniques detect material that has been plowed to the side of the sliding track as wear. Even so, wear measurements have hitherto not been able to discriminate between transferred and original material within the wear track. Additional chemical analysis can alleviate this shortcoming, but only if transferred and original materials are chemically distinct.

In this paper, we demonstrate the utility of implantation of gold atoms with a well-defined gold concentration profile into the surface, for use as markers for the determination of wear properties of an Al-Si alloy. Before and after rubbing, the profiles can be measured with electron scanning probes for the analysis of wear. This gold marker technique (henceforth denoted as GMT) has allowed us to measure wear with sub-micron spatial resolution, to distinguish transferred from original material, and in addition to visualize certain tribo-induced processes such as the rotation of Si particles in the alloy.

As an application of GMT we have studied the wear of Al-Si alloys, which offer significant mass reduction compared to ferrous alloys when used in automobile engines. The technological surface has hard silicon and intermetallic particles, which initially stand up proud of the soft aluminum matrix and are believed to carry the load in a frictional contact. This initial morphology of the surface undergoes inevitable change during motion against a counterface, the outcome ranging from catastrophic wear to moderate intermixing; these processes can result in a strong, nanocrystalline surface layer.[22] The alteration of the surface is likely to be initiated by the motion of the hard particles (Si and intermetallics) relative to the soft aluminum matrix. We demonstrate that the initial stages of these processes can be well

characterized with GMT.

GMT utilizes the quantitative implantation of gold atoms with a well-defined concentration profile into a surface, followed by the measurement of the gold concentration after rubbing. In our original experiments [23,24], analysis of the gold profiles was carried out using Rutherford backscattering spectroscopy (RBS) with the incident beam normal to the original sliding interface. In that case, the average gold concentration depth profile could be determined within a beam spot of approximately 1 mm^2. In the present paper, we use EDX as the analytical method, resulting in a spatial resolution of 0.1 microns down to a few nm, however, at the expense of reduced depth resolution. The net number of gold atoms in the irradiated zone can still be determined with high precision with EDX, allowing one to deduce wear accurately. Sub-nanometer depth resolutions can be achieved by use of cross-sectional EDX analysis in transmission mode on FIB'ed cross sections (lamellae) cut normal to the sliding interface(s). Experiments where the imaging electron beam is incident normal to the sliding interface are termed "GMT mode 1"; "GMT mode 2" refers to experiments where the electron beam is incident normal to the FIB'ed surface.

Figure 1 shows scanning transmission electron microscopy (STEM) of a lamella cut from an etched and worn sample, whose silicon grains originally protruded about 1 micron out of the surface. The Au-marked regions of Si can be distinguished from the unmarked ones due to their different contrasts in the STEM . The border between marked and unmarked Si is therefore clearly visible and allows one to deduce rubbing induced changes in the sample morphology. For example, the particle labeled (a) must have been pushed into the interface without rotation, because the contact line between Au-marked and unmarked region is parallel to the interface. Conversely, the equivalent linear feature where the contrast changes in the particle with labels (c) and (d), is tilted by 25° ± 0.5°, which is the angle by which this grain

must have rotated. The ability to determine such changes in orientation of different phases is unique to the GMT and represents an entirely new capability for the study of morphology changes in materials.

Without showing explicit evidence, we wish to note that STEM cross-sections of etched and non-etched surfaces exhibit similar characteristics after a wear experiment. Based on this observation, we conclude that the wear mechanism of etched Al-Si surfaces (in the limit of ultra-mild wear as investigated here) smoothly evolves into that of a non-etched one, specifically after the silicon particles have been pushed into the aluminum matrix and worn, forming a smooth interface with the aluminum matrix. However, less aluminum is removed during run-in of the tribo-contact when the alloy has been etched than is the case for a non-etched sample.

What cannot be learned from the STEM images alone is whether the Au-implanted aluminum has fully worn off, although this appears to be plausible from the bright contrast in the region of the Al matrix. Furthermore, it is not possible to ascertain if any rubbing-induced mixing occurred within the silicon particle. These issues can be addressed with the help of EDX measurements of the gold concentration profiles determined along selected paths by transmission STEM-EDX on the thin FIB-excised lamellae. These are shown in **Fig. 2**.

The concentration profile (b) in Figure 2, which was measured along trace (b) in Figure 1, shows conclusively that at least the full thickness (depth) of the gold-marked aluminum surface layer has been worn off. Conversely, the silicon particles contain originally Au marked material and thus they have worn distinctly less than the Al matrix (e.g. Fig. 2(a)), despite the fact that the surface of the Si particles was originally ~ 1μm above the matrix surface. In addition, the EDX signal from the worn interface can be mapped onto the original one, clearly showing that no mixing occurred within the two particles examined. One can also ascertain the wear depth quite accurately, i.e., 375 nm for the particle marked (a), and 175 nm

/ 270 nm for the other silicon particle near the front (c) / trailing edge (d). In case (d), original and measured data can be mapped onto one another by stretching / compressing the z axis by cos 25°, as alluded to in the discussion of Figure 2.

The question arises why one silicon particle rotates under sliding, while the other one does not. The answer may lie in the geometry of the particles. Their initial heights were both roughly 850 nm. However, particle (a) extends 10 microns laterally in the sliding direction (not illustrated in Fig. 1, but apparent in wider area images), while the other one is five times shorter. Thus, particle (a) had a much smaller height/width ratio making it more stable against rotation. Because the other particle has a relatively smaller cross sectional area normal to the surface, it is more easily embedded into the aluminum, thus potentially being exposed to lower frictional induced stresses which may explain why it exhibits less wear.

So far, we have focused on the wear behaviour of relatively small hard particles (i.e. silicon particles of ~2 microns), using GMT mode 2. We have not established yet if the wearing of hard particles can begin before they become embedded into the matrix. To address this question we have investigated a larger (by a factor of 10) hard Cu-Ni intermetallic particle with GMT mode 1. **Figure 3** shows an SEM image of a worn, pre-etched Al-Si interface with a damaged intermetallic particle. The circles indicate locations with corresponding residual per cent of gold, which was determined with help of EDX spectroscopy. The inset shows the spectral feature of gold (Mα1) in the EDX-spectra measured in an unworn and a worn region. The approximately 20 μm long grain has been fractured and divided into front, center and trailing edge sections. From the ≈ 25% Au concentration near the front, and the ≈ 50% Au concentration at the trailing edge, one can deduce a 200 nm wear depth difference. Assuming that the worn upper surface is parallel to the sliding interface and that no wear of the hard intermetallic occurred due to interactions with the soft aluminum matrix (both of which was

true for the silicon particles investigated above), one can conclude that the particle has only rotated by an angle of $\alpha = \sin^{-1}(200\ \text{nm}/20\ \mu\text{m}) \approx 0.6°$. Estimating the angle of rotation with the 15% Au concentration found in the center edge (which may have become the new front edge after the intermetallic particle fracture), we would estimate the rotation angle as $\alpha = \sin^{-1}(250\ \text{nm}/15\ \mu\text{m}) \approx 1°$. The result of this analysis agrees with our previous observations that (i) long grains barely rotate and (ii) wear is greater at the front than at the trailing edge of particles.

The wear and rotation of the large and hard intermetallic grain was initiated before it was fully embedded into the aluminum matrix. This can be ascertained from the relatively high Au concentration found in the aluminum matrix adjacent to the grain.

As a last application of GMT mode 1, we have investigated the wear characteristics of an unetched surface. Figure 2 SI (in the supplementary information) shows EDX elemental maps of two different locations on the surface, one containing a silicon particle and another one a hard intermetallic particle. It can be seen in both cases that the hard particles have not worn more than the implantation depth of gold, while the Au implanted zones of aluminum have been almost completely removed. Thus wear of the non-etched Al-Si surface is dominated by the wear of the aluminum matrix as has been the case for the etched surface during the later stages of wear.

In summary, we have introduced a new method of evaluating the wear of materials which affords detailed insights into plastic deformation and wear mechanisms, and yields accurate, phase-specific wear rates even in the ultra-mild wear regime. The unique capabilities of the method depend upon the quantitative implantation of gold atoms in known depth profiles. We illustrated the capabilities of GMT by experiments on an important technological alloy (Al-Si) under conditions simulating the cylinder-bore contact in an automobile engine. The data show

that the wear of an etched sample in which the silicon grains stand proud of the Al matrix by ~ 1 μm, evolves smoothly into that characteristic of an unetched sample, the major difference being the run-in period on the etched sample where the load is largely born by the Si grains. The much higher wear of the Al matrix compared to the hard phases (Si, Si-containing intermetallics) has been clearly demonstrated.

The depth- and laterally-resolved analysis of the gold profiles has demonstrated that hard particles can be individually studied, revealing their displacement into the surface (embedding under load), and rotations that depend upon the grain geometry, particularly the height-to-width ratio. Increased wear is observed at the leading edges of these phases and can be correlated with changes in particle orientation with respect to the plane of the sliding surfaces. Virtually none of these observations and conclusions would be possible without the use of GMT.

The capabilities illustrated in this paper are clearly relevant not only to nanoscale phenomena in macroscale devices and machines, as illustrated here, but also to the tribology of micro- and nanomachines.

Experimental

The cast pieces of A380 were cut into 3 mm thick squares with side dimensions of 12.7 mm. The cut samples were ground using sand paper and finally polished with 0.1 μm diamond paste. The technological surface was prepared by exposing half of the samples for 120 s to 10% NaOH solution to expose Si and other slow-etching phases so that their surfaces are elevated above the Al matrix by ~1micron.

A typical set of parameters used for the implantation in this work is the following sequence of implantation energies and fluences: 390 keV and 3.0×10^{15} atoms/cm^2; 1000 keV and 3.0×10^{15}

atoms/cm^2; and 2000 keV and 3.0×10^{15} atoms/cm^2, yielding a total fluence of 0.9×10^{16} atoms/cm^2 up to the maximum depth of 800 nm. The non-implanted samples were used to ensure that gold implantation did not change the average amount of wear, and thus by implication, that the wear mechanism was also unchanged.

"GMT mode 1" - experiments were conducted using the LEO 1540XB FIB/SEM/EDX CrossBeam system at the Nanofabrication Laboratory at the University of Western Ontario. The incident electron energy was tuned in the range between 5 to 15 keV to achieve maximum SNR when measuring gold concentration.

"GMT mode 2" - experiments were carried out using the JEOL 2010F at the Canadian Centre for Electron Microscopy, McMaster University. The orientation of the sample to the beam and incident energy (typically 30 keV) was set to meet highest SNR.

Acknowledgements
Acknowledgements appear in Supporting Information, which is available online from Wiley InterScience or from the author.

Received: Revised: Published online:

[1] Dowson, D. *Hystory of Tribology* ; Wiley-Interscience: London, New York, 1998.

[2] Gahr, K. Z. *Tribology International* 1998, *31* , 587–596.

[3] Sawyer, W. G., Freudenberg, K. D., Bhimaraj, P., Schadler, L. S. *Wear* 2003, 254, 573-580

[4] Flater, E. E., Corwin, A. D., de Boer, M. P., Carpick, R. W. *Wear* 2006, 260, 580-593

[5] Carpick, R. W., Salmeron, M, *Chemical Reviews* 1997, 97, 1163-1194

[6] Gotsmann, B., Duerig, U. T., Sills, S., Frommer, J., Hawker, C. J. *Nano Letters* 2006, 6, 296-300

[7] Gotsmann, B, Lantz, M. A. *Physical Review Letters* 2008, 101, 125501

[8] Stavinoha, L. L.; Quillian, R. D., J. *U. S. Govt. Res. Develop. Rep.* 1969, *69* , 106.

[9] Nadkarni, R. A. Symposium on Modern Instrumental Methods of Elemental Analysis of Petroleum Products, Philadelphia, PA, USA, 1991; pp 5–18.

[10] Wheeler, B. D. Symposium on Modern Instrumental Methods of Elemental Analysis of Petroleum Products, Philadelphia, PA, USA, 1991; pp 136–147.

[11] Okada, S.; Kweon, C.-B.; Foster, D. E.; Schauer, J. J.; Shafer, M. M.; Christensen, C.

G. SAE World Congress & Exhibition, March, Detroit, MI, 2003

[12] Parkinson, T. F.; Mulvaney, S. T.; Marshall, H. P.; Knight, H. G. Transactions of the American Nuclear Society, USA, 1981; p 359.

[13] Harper, W. A.; Beeley, P. A.; Bennett, L. G. I.; Page, J. A. *Journal of Radioanalytical and Nuclear Chemistry* 1989; *132* , 409–422.

[14] Netten, C. V. *Science of the Total Environment* 1999, *229* , 125–129.

[15] Lunde, G.; Anderson, P. B. *International Journal of Machine Tool Design and Research* 1970*; 10* , 79–93.

[16] Jost, K. *Automotive Engineering* 1996, *104* , 33.

[17] Jones, G. W.; Armini, A. J.; Schoen, N. C. *SAE Preprint No. 780972* 1978.

[18] Kolasinski, R. D.; Polk, J. E. 39th AIAA/ASME/SAE/ASEE Joint Propulsion Conference and Exhibit, Reston, United States, 2003

[19] Schneider, E. W.; Blossfeld, D. H. *SAE (Society of Automotive Engineers) Transactions* 1990; *99* , 2170–2179.

[20] Treuhaft, M. B.; Eberle, D. C.; Timmons, S. A.; Wendel, G. R. 2003 ASME International Mechanical Engineering Congress, 2003; pp 55–64.

[21] Scherge, M.; Pohlmann, K.; Gerve, A. *Wear* 2003, *254* , 80–117.

[22] Dienwiebel, M.; Pöhlmann, K.; Scherge, M. *Tribology International* 2007, *40* , 1597–1602.

[23] Li, Y.-R.; Shakhvorostov, D.; Pereira, G.; Lachenwitzer, A.; Lennard, W. N.; Norton, P. R. *Tribology Letters* 2008, *33* , 143–152.

[24] Li, Y.-R.; Shakhvorostov, D.; Lennard, W. N.; Norton, P. R. *Tribology Letters* 2008, *33* , 63–72.

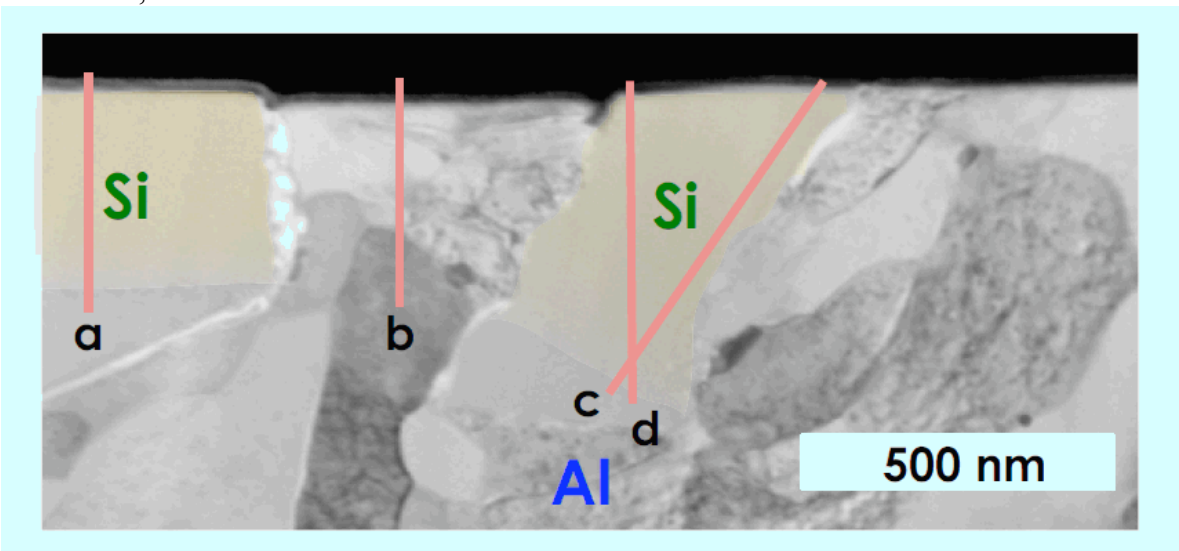

Figure 1. Scanning transmission electron image of a worn etched Al-Si alloy (focused ion beam cross section). (a-d) indicate lines, along which the Au-concentration profiles were measured (GMT mode 2). The sliding direction of the sample is from right to left with the counterface having been at the top.

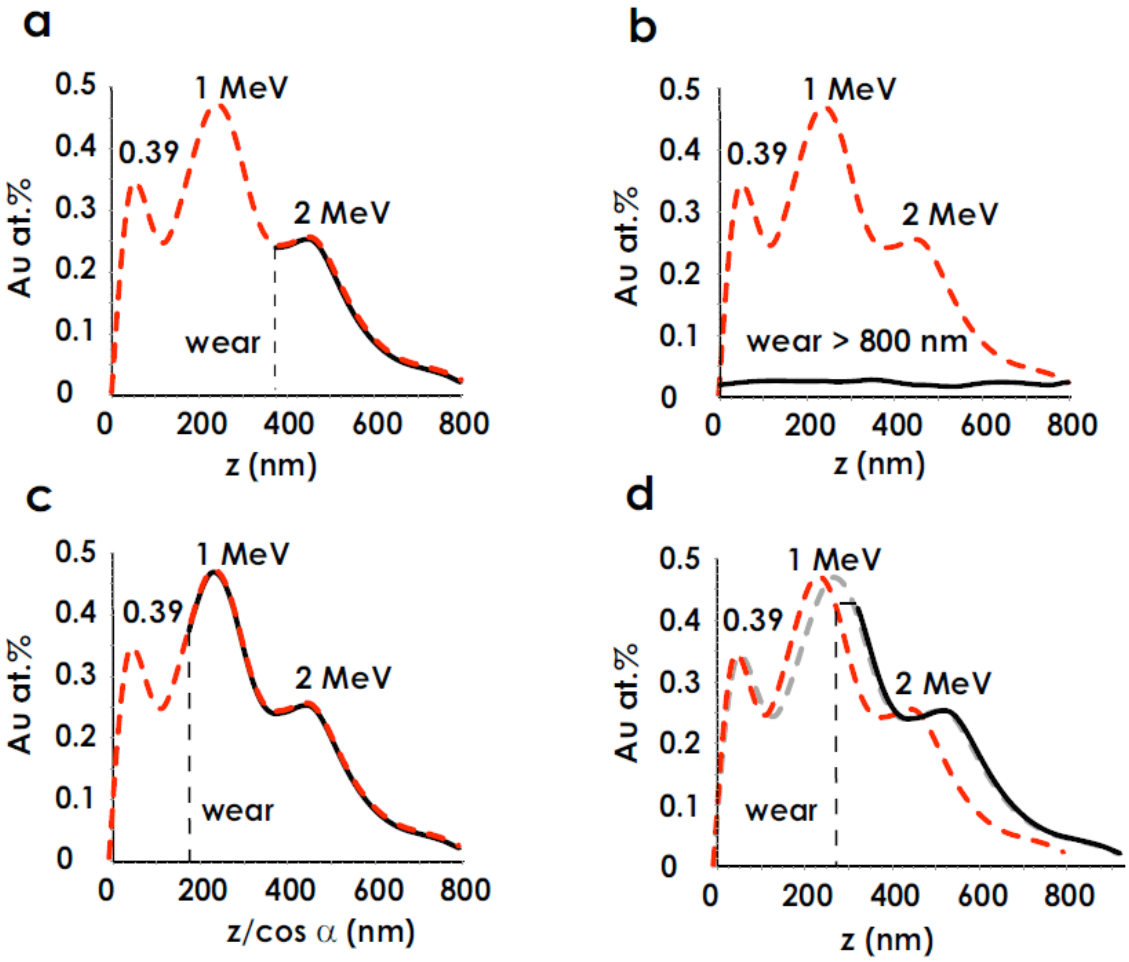

Figure 2: Gold concentration as a function of depth for different locations as determined by energy dispersive x-ray spectroscopy. The dashed lines show the original concentration, while full lines indicate the profile after rubbing. In (a,c,d) they are shifted on the z-axis to match the original concentration. Labels (a-d) are used consistently with the labels in Figure 1.

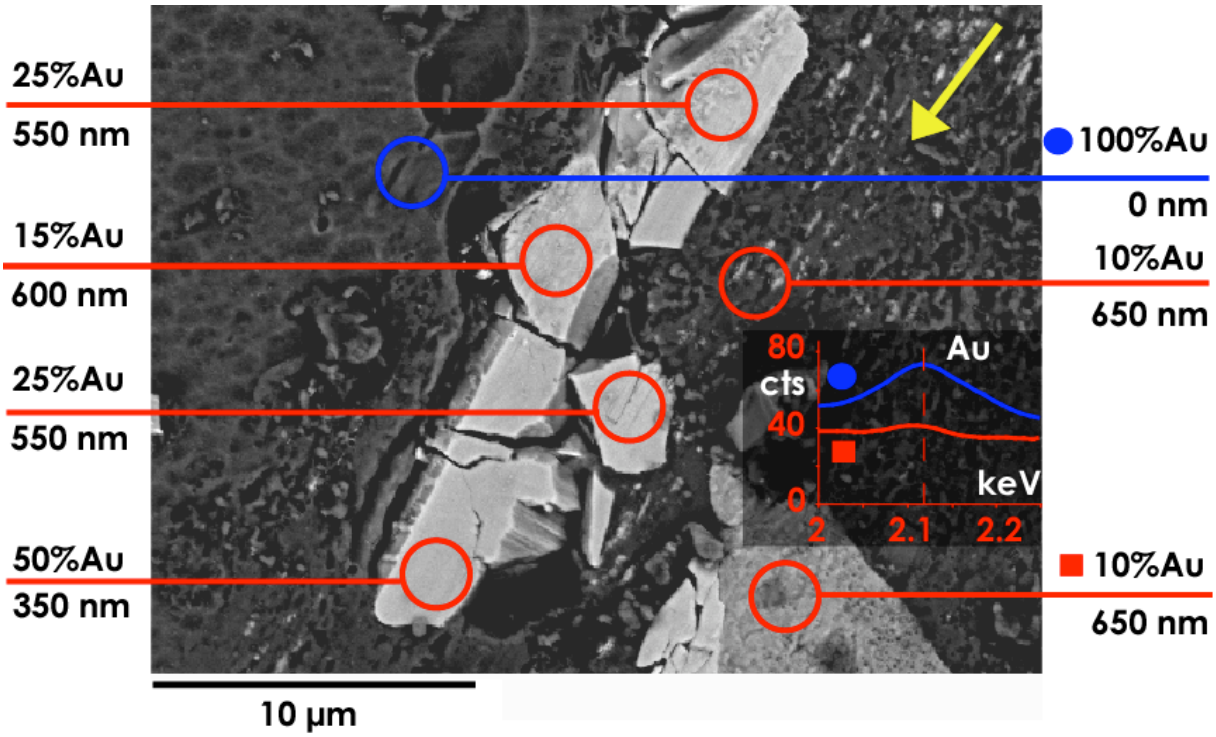

Figure 3: Scanning electron microscopy of a worn Al-Si interface with exposed Ni-containing intermetallics. Remaining per cent of gold is measured with EDX (GMT mode 1) at indicated locations. The inset shows comparison of Mα1 Au peak measured in a worn and an unworn location. Corresponding wear values are calculated using the originally implanted gold concentration profile. The yellow arrow indicates the sliding direction of the counterface.

Table of contents entry

We have developed a gold marker technique that allows one to measure wear with nanometer resolution laterally and normal to a materials surface. Owing to the analysis of gold concentration profiles before and after rubbing, the method can distinguish newly added from original material and afford information on phase-specific wear and sub-surface processes such as they occur in aluminum-silicon alloys.

Keywords: Wear, GMT, Gold Marker Technique, Aluminum-Silicon Alloy

Dmitry Shakhvorostov*, Peter R. Norton, and Martin H. Müser

A gold marker technique revealing phase-specific wear and sub-surface deformation with nanometer resolution

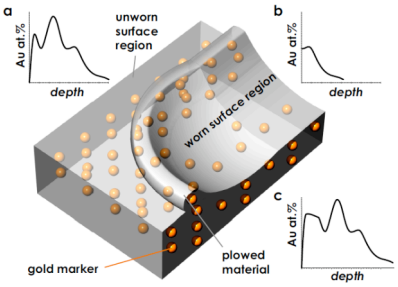

Supporting Information

Background on Al-Si alloys

Al-Si alloys and related materials can offer a significant weight saving when used for example as a sliding surface in the cylinder bores of an automobile engine, resulting in higher fuel efficiency [1]. An additional advantage related to aluminum alloys, is that they eliminate the need to install grey cast liners into the engine block; this results in reduced engine mass and energy consumption during fabrication.

When used in tribological applications, aluminum is strengthened with hard silicon grains, because pure aluminum is too soft to withstand typical tribological conditions that occur, for example, in the cylinder-bore contact [2,3,4,5,6,7]. The silicon particles in the aluminum matrix are assumed to bear the loading and sliding-induced stresses [2,3,4]. The aluminum matrix may still be easily deformed between the grains, unless the concentration of silicon significantly exceeds that of the eutectic composition. Casting alloys with such high desired silicon content requires specially designed pressure/temperature protocols [8], which increases the production expenses. As an alternative to using a high silicon content, it is possible to alloy the aluminum matrix with Cu, Mg, Mn, Ni or Cr, increasing the strength of the material through the alloying itself, as well as through binding silicon within hard intermetallic phases [9]. In order to prevent the remaining aluminum-rich phases from interacting with the counterface, surfaces are often base etched [2,3]. This makes the silicon grains and other hard, slow-etching phases of the alloy stand up proud of the aluminum matrix, and thus offer the predominant contact surface.

Experimental details

Sample preparation, gold implantation, and testing conditions

The samples were made of cast Al-Si alloy containing Si: 12.6 at%, Cu: 0.87 at%, Fe: 0.37 at%, Mn: 0.79at%, Mg: 0.26at%, Ni: 1.0at%, Ti: 0.11at%, Sr: 0.02at%, Al: Bal. The composition is close to eutectic, yielding typical and maximum grain sizes of 1 micron and 100 microns respectively.

In order to use the material in wear experiments, the cast pieces were cut into 3 mm thick squares with side dimensions of 12.7 mm. The cut samples were ground using sand paper and finally polished with 0.1 μm diamond paste. In order to investigate how etching (i.e. exposure of silicon grains) affects wear, half of the samples were not etched at all after mechanical polishing, while the other half were exposed for 120 s to 10% NaOH solution. During this process, silicon grains and intermetallic phases which etch much more slowly than the Al matrix, are exposed so that their surfaces are elevated above the Al matrix by ~1micron. Half of each of the etched and non-etched samples were implanted with gold in the implantation chamber of the Tandetron facility at the University of Western Ontario. Implantation energies and fluences were varied to obtain specific gold depth profiles (characterized by quantities such as the maximum implantation depth, average concentration of gold in the layer and the smoothness of the profile). A typical set of parameters used for the implantation in this work is the following sequence of implantation energies and fluences: 390 keV and 3.0×10^{15} atoms/cm^2; 1000 keV and 3.0×10^{15} atoms/cm^2; and 2000 keV and 3.0×10^{15} atoms/cm^2, yielding a total fluence of 0.9×10^{16} atoms/cm^2 up to the maximum depth of 800 nm.

The non-implanted samples were used to ensure that gold implantation did not change the amount of wear, and thus by implication, that the wear mechanism was also unchanged. This check was achieved successfully within the statistical noise by comparing the wear of marked and unmarked samples with neutron activation analysis (NAA) of the effluent lubricant. Despite this positive result, we would like to point out that gold implantation amorphizes the near-surface region of the silicon particles, which in principle could affect the wear mechanism. However, we never observed any effect attributable to amorphization (wear was not a function of total fluence) and therefore believe that implanted samples afford reliable wear data. We note that both crystalline and amorphous silicon are both distinctly stiffer and harder than the aluminum matrix. In future experiments, we will reverse the implantation-induced amorphization of the silicon by means of laser surface recrystallization as used in the semiconductor industry [10].

The as-prepared aluminum-silicon samples were rubbed against a steel counterface using constant normal force (6 N) and sliding velocity (0.25 m/s) using a flat-on-flat contact geometry for 0.5, 1, 5, 15, and 30 minutes, after which they were rinsed with hexane to remove the residual lubricant (fully formulated Mobil 1 engine oil) and then cleaned in an ultra-sonic bath with acetone. After the cleaning procedures the samples were analyzed with scanning electron microscopy (SEM) and prepared for transmission electron microscopy using focused ion beam (FIB) milling.

Wear determination via gold markers

The principle of wear determination with GMT providing sub-surface information, is explained in **Figure 1 SI**, which shows a schematic of the end of a wear track produced by a spherical asperity. In our example, there are (a) unworn and (b) worn regions as well as (c)

areas with deposited material that was ploughed from the wear track. For a system resembling the schematic, one could cut the sample at its centre with a focused ion beam and measure the gold concentration $C(z)$ as function of depth z by energy dispersive X-ray spectroscopy (EDX) from the side. As will be described in the next paragraph, this procedure will allow one to gain insight into the wear mechanism.

The various profiles that one might expect to observe in our example are:

(a) $C(z)$ remains unchanged.

(b) $C(z)$ is shifted towards the surface, and any signal for $z < 0$ lost. Mathematically, one could express this with the following transformation $C(z) \rightarrow \Theta(z)C(z+\Delta z)$, where $\Theta(z)$ is the Heaviside step function and Δz is the depth of the wear track.

(c) $C(z)$ is shifted away from the surface and material added on top. Hence $C(z) \rightarrow C(z+\Delta z)+C_{new}(z)$, where C_{new} depends on the gold concentration in the material displaced to that position. Here $\Delta z < 0$ is considered a negative wear.

In addition (not shown in the qualitative figure, but further discussed in the results section of the manuscript), stiff grains could be rotated, resulting in a stretched concentration profile, e.g., when the rotation angle is α then (d) $C(z) \rightarrow C(z \cdot \cos\alpha)$. If a single one of these four processes dominates, then it is relatively simple to identify that process. If however, combinations of these processes occur, then it will probably be difficult to ascertain if the original material was simply mixed and/or original material was removed and replaced with new marked material.

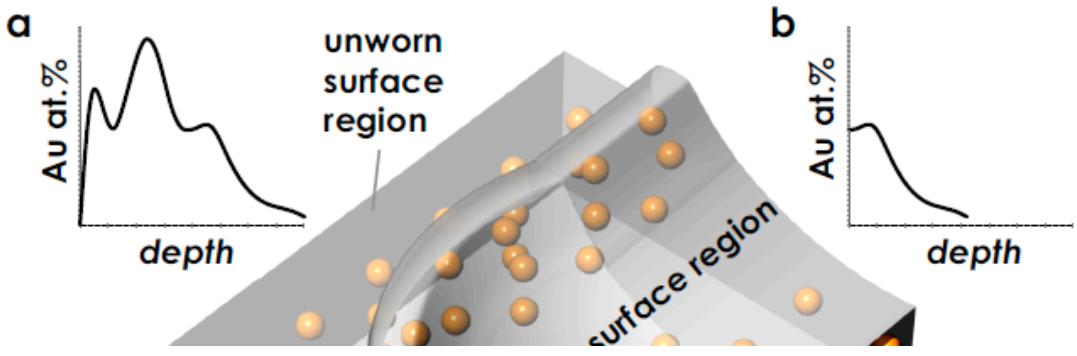

Figure 1 SI: Schematic view of the gold-implanted surface after a sliding contact with an asperity. Shown are gold depth profiles of (a) worn and (b) unworn regions, as well as (c) regions with deposited material on top. The unworn region is used as a reference. Linear wear can be obtained via the evaluation of gold concentration as shown in the schematic concentration profiles.

Scanning electron microscopy (SEM) and energy dispersive X-ray spectroscopy (EDX) in GMT mode 1

For GMT mode 1, we have used scanning electron microscopy to image the surface and at the same time combined it with EDX to measure the gold concentration and, if desired, that of other elements. The high atomic mass of gold atoms is the reason why gold markers can be detected down to 0.1at.% in our samples. The lateral resolution is typically in the order of 0.1-1 micron depending on the incident energy of the imaging electrons. This limit results from the scattering of electrons within the irradiated material and cannot be further reduced significantly with the currently available techniques.

The higher the energy of the incident electrons, the higher is their penetration depth λ_e, which should be on the order of the maximum implantation depth of Au λ_{Au}. The optimum value for λ_e depends on the details of the implantation profile. Choosing λ_e much larger than λ_{Au} reduces the signal to noise ratio, while small values of λ_e makes the result insensitive to the tails of the concentration profiles. This in turn would lead to an underestimate of the gold concentration, in particular for an unworn surface. By integrating the originally implanted gold depth concentration profile and dividing it by the total fluence, a calibration curve can be obtained, which is used to transform the fraction of removed gold into the wear depth [11,12].

In our study, λ_{Au} was less than 800 nm. We tuned λ_e between 100 and 800 nm by changing the electron energy from 5 to 15 keV. Experiments were conducted using the LEO 1540XB FIB/SEM/EDX CrossBeam system at the Nanofabrication Laboratory at the University of Western Ontario.

Scanning transmission electron microscopy (STEM) and EDX in GMT mode 2

In order to obtain information about the presence of gold as a function of depth, a cross section of the near surface region was cut out with a focused ion beam. STEM was then used to image the cross section and at the same time combined with EDX to measure the concentration of gold and any other elements of interest as a function of depth into the sample.

STEM measures the electron transmission, which is strongly reduced by the presence of gold due to its large scattering cross section. This allows one to quickly acquire an area map. EDX spectra accumulate more slowly than STEM images, which is why EDX is typically only done as a line scan, the location of which may be chosen from information provided by the STEM image. Our measurements were carried out using the JEOL 2010F at the Canadian Centre for Electron Microscopy, McMaster University.

“GMT mode 1” observations on polished surfaces

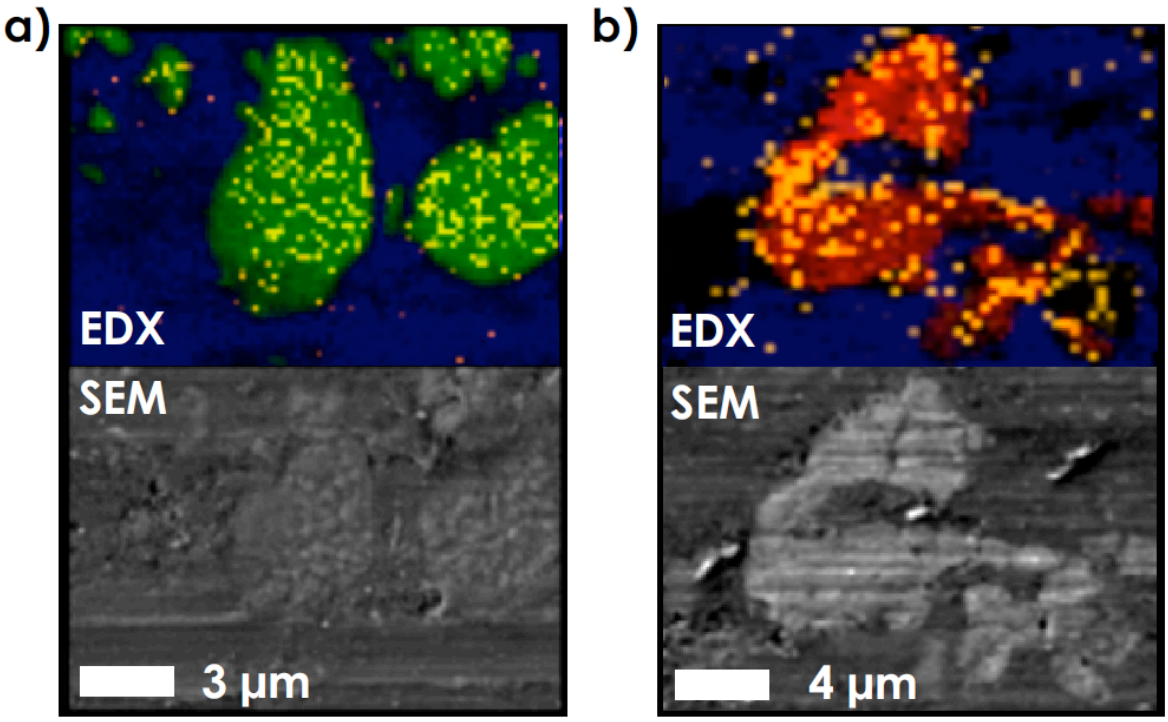

Figure 2 SI: Elemental EDX-maps (Aluminum -blue, Silicon -green, Iron -red, Gold -yellow) and corresponding scanning electron microscopy(SEM) of the worn locations. Gold markers are retained in mechanically stable phases -silicon (a) and iron containing intermetallic phase (b).

Figure 2 SI shows EDX elemental maps of two different locations on the surface, one containing a silicon grain and another one a hard intermetallic grain. It can be seen in both cases that the hard grains have not worn more than the implantation depth of gold, while the Au implanted zones of aluminum have been almost completely removed. Thus wear of the non-etched Al-Si surface is dominated by the wear of the aluminum matrix as has been the case for the etched surface during the later stages of wear.

Acknowledgement

The authors would like to thank Mr. Sanjib Day (Univsersity of Windsor) for providing worn etched Al-Si samples, Prof. A. Alpas (University of Windsor) and Mr. T. Perry (General

Motors R&D Center, Warren) for useful discussions, Mr. Phil Shaw and Mr. Brian Dalrymple of the Physics Machine Shop for help in sample preparation and Dr. Leighton Coatsworth (all from UWO) for useful discussions. We are also grateful to Mr. Jack Hendricks for operation of the Tandetron accelerator and to Dr. Todd Simpson for expertise and useful discussions regarding the SEM/EDX analysis, Nanofab University of Western Ontario. We want to acknowledge Fred Pearson (The Canadian Centre for Electron Microscopy, McMaster University) for expertise and useful discussions regarding the TEM/EDX analysis. This work was financially supported by the Natural Sciences and Engineering Research Council of Canada (NSERC), General Motors of Canada Ltd., and General Motors R&D Center.

References

[1] Hosking, F. M, Portillo, F. F., Wunderling, R., Mehrabian, R. *Journal of Materials Science* 1982, 17, 477-498

[2] Chen, M.; Alpas, A. T.; Perry, T. *Wear* 2007, *263* , 552–561.

[3] Chen, M.; Meng-Burany, X.; Alpas, A. T.; Perry, T. A. *Acta Materialia* 2008, *56* , 5605–5616.

[4] Dienwiebel, M.; Pöhlmann, K.; Scherge, M. *Tribology International* 2007, *40* , 1597–1602.

[5] Elmadagli, M.; Alpas, A. T.; Perry, T. *Wear* 2007, *262* , 79–92.

[6] Pereira, G.; Lachenwitzer, A.; Kasrai, M.; Norton, P. R.; Capehart, T. W.; Perry, T. A.; Cheng, Y. T.; Frazer, B.; Gilbert, P. U. P. A. *Tribology Letters* 2007, *26* , 103–117.

[7] Wilson, S.; Alpas, A. T. *Wear* 1997, *212* , 41–49.

[8] Yamagata, H.; Kasprzak, W.; Aniolek, M.; Kurita, H.; Sokolowski, J. *Journal of Materials Processing Tech.* 2008, *203* , 333–341.

[9] Kaufman, J.; Rooy, E. *Aluminum Alloy Castings: Properties, Processes, and Applications*; ASM International: Materials Park, OH, 2004.

[10] Geiler, H. *Materials Science Forum* 2008, 573-574 , 237–256.

[11] Li, Y.-R.; Shakhvorostov, D.; Pereira, G.; Lachenwitzer, A.; Lennard, W. N.; Norton, P. R. *Tribology Letters* 2008, *33* , 143–152.

[12] Li, Y.-R.; Shakhvorostov, D.; Lennard, W. N.; Norton, P. R. *Tribology Letters* 2008, *33* , 63–72.